arXiv:0912.1117v2 [cond-mat.quant-gas] 1 Apr 2010

Diffusion of cold atomic gases in the presence of an optical speckle potential

L. Beilin, E. Gurevich and B. Shapiro

Department of Physics, Technion - Israel Institute of Technology, Haifa 32000, Israel

Abstract

We consider diffusion of a cold Fermi gas in the presence of a random optical speckle potential. The evolution of the initial atomic cloud in space and time is discussed. Analytical and numerical results are presented in various regimes. Diffusion of a Bose-Einstein condensate is also briefly discussed and similarity with the Fermi gas case is pointed out.

I. INTRODUCTION

Transport of cold atomic gases in the presence of a quenched random potential is a rapidly developing field of research [1]. In a typical set-up the gas is released from a harmonic trap and undergoes expansion, while being scattered by the random potential. At some later time an image of the expanded atomic cloud is taken and, thus, information about the mode of transport (ballistic, diffusive or localized) is obtained. The random potential for atoms is obtained by creating a random pattern of light intensity (optical speckle). Experiments on propagation of cold atoms through optical speckles have been limited so far to one-dimensional ($1d$) geometry and have culminated in observation of $1d$ Anderson localization for a Bose-Einstein condensate (BEC) [2, 3].

There is a considerable amount of theoretical work on diffusion and possible localization of an expanding BEC cloud in two and three dimensions [4–9]. The same problem can be also addressed for a cold Fermi gas - a system which is intensively studied in recent years (see [10, 11] for recent reviews). Diffusion of an expanding Fermi gas, in the long time limit and for a Gaussian white noise potential, was discussed in [12]. In the present paper we consider the experimentally relevant case of a speckle potential, concentrating on $2d$ geometry. In Sec. II we write down the basic equations which govern the evolution of a diffusing Fermi cloud. In Sec. III we summarize, following [13], the behavior of the diffusion coefficient $D(k)$, as a function of the particle wave number k, in a $2d$ speckle potential. In Sec. IV we study the density $n(\vec{r},t)$ of a diffusing Fermi gas as a function of position and time. Since $n(\vec{r},t)$ is expressed by an integral which cannot be calculated analytically, we resort to numerics in combination with an analytic treatment of some limiting cases. In Sec. V we briefly discuss the evolution of the shape of a diffusing BEC and point out some similarities (and differences) with the case of the Fermi gas.

II. BASIC EQUATIONS

We consider N fermions at zero temperature, initially trapped in a harmonic potential. At time $t = 0$ the trap is switched off, while a random potential $V(\vec{r})$ is switched on. Our aim is to study the dynamics of the atoms, upon their release from the trap, in the presence of the random potential. In many circumstances interactions between the fermions have only a minor effect on their dynamics. This is particularly true for a polarized Fermi gas when the Pauli principle eliminates the main mechanism (the s-scattering) for the interaction. In the absence of interactions the single particle wave functions, $\Psi_n(\vec{r},t)$, describing individual atoms, evolve according to:

$$i\hbar\partial_t\Psi_n(\vec{r},t) = -\frac{\hbar^2}{2m}\triangle\Psi_n(\vec{r},t) + V(\vec{r})\Psi_n(\vec{r},t)\ , \tag{1}$$

with the initial condition $\Psi_n(\vec{r},0) = \Phi_n(\vec{r})$, where $\Phi_n(\vec{r})$ is n'th eigenstate of the harmonic potential $\frac{1}{2}m\omega^2r^2$, and $V(\vec{r})$ is the random potential, with zero mean and a two-point correlation function $\langle V(\vec{r}_1)\,V(\vec{r}_2)\rangle = \Gamma(\vec{r}_2 - \vec{r}_1)$.

The formal solution of (1) is

$$\Psi_n(\vec{r},t) = \int d\vec{R}G(\vec{r},\vec{R},t)\Phi_n(\vec{R})\ , \tag{2}$$

where $G(\vec{r},\vec{R},t)$ is the retarded Green's function of the Schrödinger equation (1). The quantum expectation value of the particle density (per one spin component) at time t and for a given realization of randomness is

$$< \hat{n}(\vec{r},t) >= \sum_n f_n\left|\Psi_n(\vec{r},t)\right|^2 = \int d\vec{R}d\vec{R}'G^*(\vec{r},\vec{R},t)G(\vec{r},\vec{R}',t)\sum_n f_n\Phi_n^*(\vec{R})\Phi_n(\vec{R}')\ , \tag{3}$$

where f_n is the occupation function, which for zero temperature is given by the step function $\Theta(E_F - E_n)$. Averaging $< n(\vec{r},t) >$ over the disorder yields

$$< \overline{\hat{n}(\vec{r},t)} >= \int d\vec{R}d\vec{R}'\overline{G^*(\vec{r},\vec{R},t)G(\vec{r},\vec{R}',t)}\sum_n f_n\Phi_n^*(\vec{R})\Phi_n(\vec{R}')\ . \tag{4}$$

In order to average the product of the two Green's functions in (4) we first Fourier transform to the energy representation

$$\overline{G^*(\vec{r},\vec{R},t)G(\vec{r},\vec{R}',t)} = \int\frac{d\varepsilon}{2\pi}\int\frac{d\Omega}{2\pi}e^{-\frac{i\Omega t}{\hbar}}\overline{G^*(\vec{r},\vec{R},\varepsilon+\frac{1}{2}\Omega)G(\vec{r},\vec{R}',\varepsilon-\frac{1}{2}\Omega)}\ . \tag{5}$$

The product in r.h.s. of (5), in the diffusion approximation, is represented diagrammatically in Fig.1.

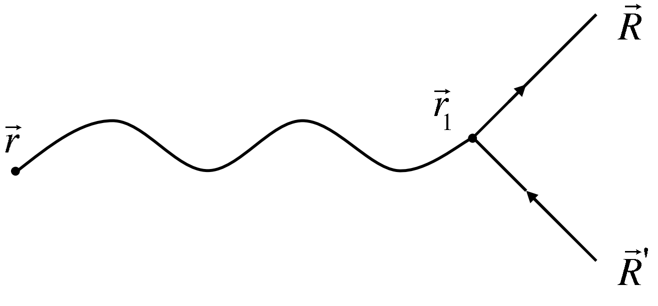

Figure 1: Diagrammatic representation of the product in Eq.(5).

The two straight lines represent a wave and its complex conjugate propagating from their sources ($\vec{R}'$ and $\vec{R}$) to an intermediate point $\vec{r}_1$. At this point the two waves "recombine" and the wave intensity propagates by diffusion to the observation point $\vec{r}$. The corresponding algebraic expression is

$$\overline{G^*(\vec{r},\vec{R},\varepsilon+\frac{1}{2}\Omega)G(\vec{r},\vec{R}',\varepsilon-\frac{1}{2}\Omega)} = \frac{\hbar}{\tau_\varepsilon}\int d\vec{r}_1 P_\varepsilon(\vec{r},\vec{r}_1,\Omega)\overline{G^*}(\vec{r}_1-\vec{R},\varepsilon+\frac{1}{2}\Omega)\overline{G}(\vec{r}_1-\vec{R}',\varepsilon-\frac{1}{2}\Omega), \tag{6}$$

where τ_ε is the scattering mean free time at energy ε, $P_\varepsilon(\vec{r},\vec{r}_1,\Omega)$ is the diffusion ladder[14] and $\overline{G}(\vec{r},\varepsilon)$ is the average Green's function. For the latter Ω can be neglected, in comparison with ε, and its explicit expression is

$$\overline{G}(\vec{r},\varepsilon\pm\frac{1}{2}\Omega) \approx \overline{G}(\vec{r},\varepsilon) = G_0(\vec{r},\varepsilon)e^{-\frac{r}{2l_\varepsilon}} \quad , \tag{7}$$

where G_0 is the free Green's function and l_ε is the single particle mean free path. Since the Green's functions in Eq.(6) rapidly decay (at a distance l_ε), the slow varying diffusion ladder $P_\varepsilon(\vec{r},\vec{r}_1,\Omega)$ can be taken out of the integral, with the argument $\vec{r}_1$ being replaced by $\frac{\vec{R}+\vec{R}'}{2}$. Performing the remaining integral and returning to (5) yields

$$\overline{G^*(\vec{r},\vec{R},t)G(\vec{r},\vec{R}',t)} = -\frac{1}{\pi}\int d\varepsilon P_\varepsilon\left(\vec{r},\frac{\vec{R}+\vec{R}'}{2},t\right) Im\overline{G}\left(\vec{R}-\vec{R}',\varepsilon\right) \ , \tag{8}$$

where the diffusion propagator

$$P_\varepsilon(\vec{r},\vec{R},t) = \frac{1}{(4\pi D_\varepsilon t)^{d/2}}\exp\left(-\frac{\left|\vec{r}-\vec{R}\right|^2}{4D_\varepsilon t}\right) \tag{9}$$

is the Fourier transform of $P_\varepsilon(\vec{r},\vec{R},\Omega)$ and D_ε is the diffusion coefficient at energy ε. The necessary condition for the above derivation is $kl_\varepsilon \gg 1$, where $k=\sqrt{2m\varepsilon/\hbar^2}$.

Substituting (8) into (4) and using the fact that for weak disorder $-\frac{1}{\pi}Im\overline{G}(\vec{k},\varepsilon) \simeq \delta(\varepsilon-\varepsilon_k)$ one obtains

$$<\overline{\hat{n}(\vec{r},t)}> \equiv n(\vec{r},t) = \int d\vec{R}\int d\vec{p}P_p(\vec{r},\vec{R},t)\sum_n f_n W_n(\vec{p},\vec{R}) \ , \tag{10}$$

where P_p is given by (9) with $\varepsilon=\frac{p^2}{2m}$ and

$$W_n(\vec{p},\vec{R}) \equiv \frac{1}{(2\pi\hbar)^d}\int d\vec{\rho}e^{\frac{i}{\hbar}\vec{p}\vec{\rho}}\Phi_n^*(\vec{R}+\frac{1}{2}\vec{\rho})\Phi_n(\vec{R}-\frac{1}{2}\vec{\rho}) \tag{11}$$

is the Wigner transform of $\Phi_n(\vec{r})$. In the classical limit ($n \gg 1$) the Wigner function $W_n(\vec{p},\vec{R})$ for an eigenstate n becomes [15]

$$W_n(\vec{p},\vec{R}) = \frac{1}{(2\pi\hbar)^d \nu(E_n)} \delta(E_n - \frac{p^2}{2m} - \frac{1}{2} m\omega^2 R^2)\,, \tag{12}$$

where E_n is the energy of state n and $\nu(E_n)$ is the density of states for a particle in a harmonic trap. Substituting this into (10) and replacing summation over n by integration over energy up to the Fermi energy E_F we finally obtain

$$n(\vec{r},t) = \int d\vec{R} \int \frac{d\vec{p}}{(2\pi\hbar)^d} P_p(\vec{r},\vec{R},t) \Theta(E_F - \frac{p^2}{2m} - \frac{1}{2} m\omega^2 R^2). \tag{13}$$

III. DIFFUSION COEFFICIENT IN SPECKLE DISORDER

In order to proceed with the evaluation of the integral in (13), an explicit expression is required for the diffusion coefficient

$$D(k) = \frac{\hbar k l_B}{dm}\,, \tag{14}$$

where l_B is the Boltzmann transport mean free path and $k = \frac{p}{\hbar}$. So far we have not specified the type of disorder. Now we specialize to a two-dimensional ($d = 2$) speckle potential, generated by transmitting laser light through circular diffusive plate, whose two-point correlation function is given by [5]

$$\Gamma(\vec{r}_1 - \vec{r}_2) = 4V_0^2 \left[\frac{J_1(k_0 \left|\vec{r}_1 - \vec{r}_2\right|)}{k_0 \left|\vec{r}_1 - \vec{r}_2\right|} \right]^2\,, \tag{15}$$

where J_1 is the first-order Bessel function, V_0 is the standard deviation and k_0 is the inverse correlation length of the random potential. The latter is related to the laser wavelength and numerical aperture of the imaging device. Then, in the weak disorder limit, the mean free path is given by [13]

$$\frac{1}{k l_B} = \eta^2 \left(\frac{k_0}{k}\right)^2 \int\limits_0^{2\pi} \frac{1}{2\pi} d\theta \widetilde{\Gamma}\left(2\frac{k}{k_0}\left|\sin\left(\frac{\theta}{2}\right)\right|\right)(1 - \cos(\theta))\,, \tag{16}$$

where $\eta = \frac{V_0}{E_0}$ is the measure of the potential fluctuations strength, $E_0 = \frac{\hbar^2 k_0^2}{m}$ is the "correlation" energy and

$$\widetilde{\Gamma}(\kappa) = 8\left(\arccos\left(\frac{\kappa}{2}\right) - \frac{\kappa}{2}\sqrt{\left(1 - \left(\frac{\kappa}{2}\right)^2\right)}\right)\Theta(2-\kappa)\,. \tag{17}$$

In the limiting cases, $k \ll k_0$ and $k \gg k_0$, (16) may be approximated as [13]:

$$kl_B \approx \begin{cases} \frac{1}{4\pi\eta^2}\left(\frac{k}{k_0}\right)^2 & , \quad k \ll k_0 \\ \frac{45\pi}{128\eta^2}\left(\frac{k}{k_0}\right)^5 & , \quad k \gg k_0 \end{cases} . \tag{18}$$

In Fig. 2(a) we compare approximations (18) to the exact numerical evaluation of (16). The optimal choice of a point, separating between the two asymptotics, is the crossing point $k_{cr} = \lambda k_0$, with $\lambda = \left(\frac{32}{45\pi^2}\right)^{1/3} \approx 0.41$. With this choice (16) is approximated as:

$$kl_B = \begin{cases} \frac{1}{4\pi\eta^2}\left(\frac{k}{k_0}\right)^2 & , \quad k < \lambda k_0 \\ \frac{45\pi}{128\eta^2}\left(\frac{k}{k_0}\right)^5 & , \quad k > \lambda k_0 \end{cases} . \tag{19}$$

The approximation (19) differs from the exact numerical solution of (16) by a numerical factor of order unity. This is demonstrated in Fig. 2(b), which shows the ratio between the two.

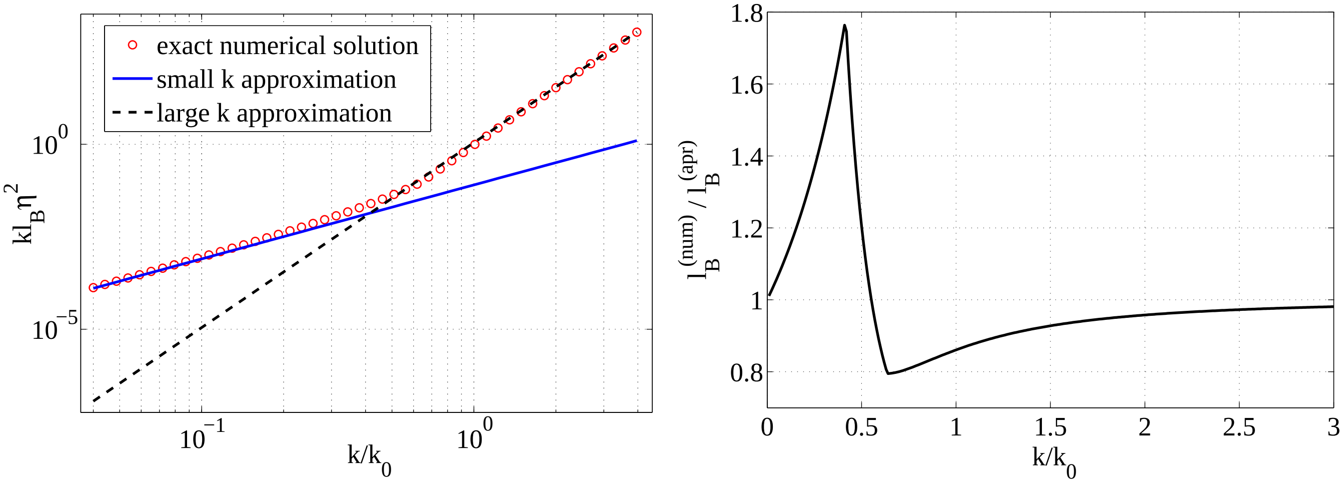

(a)

(b)

Figure 2: (Color online) (a) Comparison between the numerical (○), Eq.16, and approximate (lines), Eq.19, solution for the Boltzmann transport mean free path l_B. The small k (solid line) and large k (dashed line) asymptotics cross at $k_{cr} = \lambda k_0$; (b) The ratio between the exact numerical solution of (16) and the approximate expression (19). The maximal deviation, obtained at the crossing point $k_{cr} = \lambda k_0$, is about 1.76.

Thus, we write the diffusion coefficient as

$$D(k) = \begin{cases} D_<(k) = \frac{D_0}{8\pi}\left(\frac{k}{k_0}\right)^2 & , \quad k_c < k < \lambda k_0 \\ D_>(k) = \frac{45\pi D_0}{256}\left(\frac{k}{k_0}\right)^5 & , \qquad k > \lambda k_0 \end{cases} , \tag{20}$$

where $D_0 \equiv \frac{\hbar^5 k_0^4}{m^3 V_0^2}$. Note that we have introduced a lower cutoff k_c, which is derived from the Ioffe-Regel criterion $k_c l_B = 1$ (see below). For $k < k_c$ the diffusion approximation employed in this paper is not valid any more: thus, particles with $k < k_c$ remain localized in the vicinity of the initial trap.

IV. EVOLUTION OF THE DENSITY IN SPACE AND TIME

Using the above explicit expression for the diffusion coefficient, one can calculate the atomic density profile $n(\vec{r}, t)$ (13). It is convenient to introduce the following dimensionless variables:

$$\begin{cases} \widetilde{r} = \frac{r}{R_{Max}} \\ \widetilde{t} = \frac{t}{t_0} \\ \widetilde{n} = n R_{Max}^2 \end{cases} , \tag{21}$$

where $R_{Max} = \sqrt{\frac{2E_F}{m\omega^2}} = \frac{\sqrt{8N}}{k_F}$ is the initial size of the atomic cloud and $t_0 = \frac{R_{Max}^2}{D_0} = \frac{2\eta^2\sqrt{2N}}{\omega}$ is a characteristic diffusion time. Let us note that for $t \to 0$ the diffusion kernel (9) becomes a delta function $\delta(\vec{r} - \vec{R})$ and the density approaches its initial shape of the inverted parabola,

$$\widetilde{n}_0(\widetilde{r}, 0) = \frac{2N}{\pi}(1 - \widetilde{r}^2) , \tag{22}$$

which corresponds to the Thomas-Fermi approximation for N fermions in the harmonic trap. Since it is difficult to calculate analytically the integral in the expression (13), below we consider various special cases.

In the long time limit the atomic cloud will spread to a distance much larger than its initial size R_{Max}. Then, one can set $R = 0$ in the diffusion kernel in (13) and integrate over $\vec{R}$, with the following result:

$$n(\vec{r}, t) = \int \frac{d\vec{p}}{(2\pi\hbar)^2} P_p(\vec{r}, 0, t) \left|\widetilde{\Phi}(p)\right|^2 , \tag{23}$$

where

$$\left|\widetilde{\Phi}(p)\right|^2 = \pi R_{Max}^2 \left(1 - \frac{p^2}{p_F^2}\right) \Theta\left(p_F - p\right) \tag{24}$$

is the momentum distribution of the gas. Eq. (23) has a simple interpretation: it describes classical diffusion of particles with momentum $\vec{p}$ and energy $\varepsilon = \frac{p^2}{2m}$ and with a momentum dependent diffusion coefficient given in (20). It is interesting to note that (23) is completely analogous to the corresponding expression for a diffusing BEC, with $k_F = p_F/\hbar$ being replaced by the inverse healing length $1/\xi$ [4, 5].

The integral in (23) cannot be calculated analytically due to the complicated dependence of the diffusion kernel on the particle momentum p. A considerable simplification occurs if one assumes $p_F \ll \hbar k_0$. In this case all atomic wave numbers satisfy the condition $k < k_0$ so that correlations in the random potential do not come into play. The diffusion coefficient is given by $D_<(k)$ (see (20)) in the whole range of integration which corresponds to the limit of an uncorrelated, white-noise potential. The expression (23) reduces to:

$$n(r,t) = \frac{R_{Max}^2}{8\pi t} \int_{k_c}^{k_F} \frac{kdk}{D_<(k)} \exp\left(-\frac{r^2}{4D_<(k)t}\right)\left(1 - \frac{k^2}{k_F^2}\right). \tag{25}$$

Let us stress that the white noise limit, Eq. (25), requires that the typical strength V_0 of the random potential must be smaller than the correlation energy E_0, so that the parameter $\eta = \frac{V_0}{E_0} \ll 1$ [5]. Indeed, the white noise condition, $k \ll k_0$, is compatible with the weak disorder requirement, $kl_B > 1$, only if $\eta \ll 1$ (see (19)). This inequality implies $k_c = \sqrt{4\pi\eta}k_0 \ll k_0$. Furthermore, in order for the weak disorder requirement to be satisfied for the great majority of the fermions, we must require $k_F \gg k_c$, i.e. $E_F \gg \frac{V_0^2}{E_0}$. Switching to the dimensionless variables and performing the integral yields:

$$\widetilde{n}(\widetilde{r},\widetilde{t}) = \frac{2Ns}{\widetilde{t}}\left[-e^{-\frac{\pi s \widetilde{r}^2}{\widetilde{t}}} + 2\pi s\eta^2 e^{-\frac{1}{\eta^2}\frac{\widetilde{r}^2}{2\widetilde{t}}} + \left(1 + \frac{\pi s\widetilde{r}^2}{\widetilde{t}}\right)\left(E_1\left[\frac{\pi s\widetilde{r}^2}{\widetilde{t}}\right] - E_1\left[\frac{\widetilde{r}^2}{2\eta^2\widetilde{t}}\right]\right)\right], \tag{26}$$

where $s = \frac{E_0}{E_F}$ and the special function $E_1(x)$ is the exponential integral [16]. The aforementioned condition $E_F \gg \frac{V_0^2}{E_0}$ implies that the parameter $s\eta^2 \ll 1$. As an experimentally relevant example, we consider the Li^6 atoms in the isotropic trap with the harmonic confinement frequency $\frac{\omega}{2\pi} \approx 160\,Hz$ and the speckle scale $\frac{2\pi}{k_0} = 0.5\mu m$. For $\eta = 0.05$ and $s = 12$, this corresponds to $N \sim 10^4$ atoms trapped in the initial cloud of the radius $R_{max} \sim 50\mu m$ and the typical time $t_0 \sim 0.7ms$, which is about two orders of magnitude larger than the Boltzmann transport mean free time τ_B. Expression (26) is plotted in Fig. 3 for s and η specified above. In Fig. 3(a) $\widetilde{n}(\widetilde{r},\widetilde{t})/N$ is shown as a function of normalized time and distance. The chopped part of the plot corresponds to the region where the approximation of long time limit is not valid. Fig. 3(b) depicts snapshots of the density at different times.

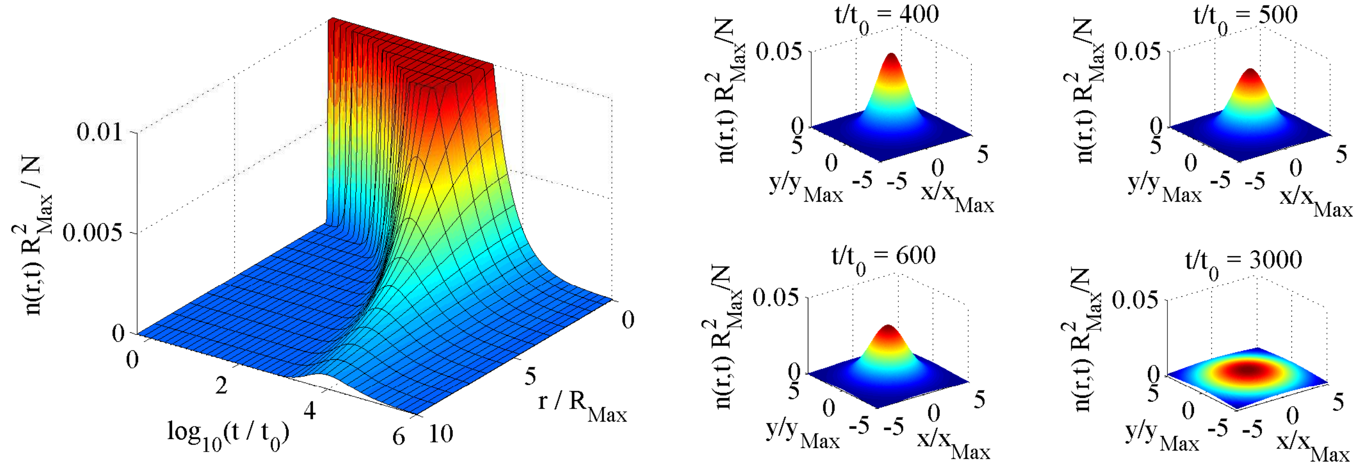

(a) (b)

Figure 3: (Color online) (a) Normalized atomic density $\widetilde{n}(\widetilde{r},\widetilde{t})/N$ Eq.(26), as a function of normalized time and distance for $s = 12$ and $\eta = 0.05$. The chopped part of the plot corresponds to small times and $\widetilde{r}$ for which the approximation of long time limit is not valid; (b) snapshots of the density for $s = 12$ and $\eta = 0.05$ at four times $\frac{t}{t_0} = 400, 500, 600, 3000$.

Let us discuss the obtained expression (26) in different regimes. For $r \lesssim R_{Max}$ (i.e. $\widetilde{r} \lesssim 1$) and for large times $\widetilde{t} > \frac{1}{\eta^2}$, using the expansion of $E_1(x)$ for small values of x [16]

$$E_1(x) = -\ln x + O(1)\,, \tag{27}$$

Eq.(26) simplifies to

$$\widetilde{n}(\widetilde{r},\widetilde{t}) \approx \frac{2Ns}{\widetilde{t}} \ln\left[\frac{1}{2\pi s\eta^2}\right]. \tag{28}$$

In the main region, $R_{Max} < r < \sqrt{4D_<(k_F)t}$ (i.e. $1 < \widetilde{r} < \sqrt{\frac{\widetilde{t}}{\pi s}}$), expression (26) is not intuitive and, for the visualization, in Fig. 4 we compare it with the solution for constant $D = D_<(k_F)$(see Eq.(20))

$$\widetilde{n}(\widetilde{r},\widetilde{t}) = \frac{Ns}{\widetilde{t}} e^{-\frac{\pi s \widetilde{r}^2}{\widetilde{t}}}(1 - 2\pi s\eta^2)^2, \tag{29}$$

where the factor in the parentheses accounts for the lower momentum cutoff k_c. As expected, the solution for $2d$ speckle has a more compact shape and the density decays faster than in the case of constant D, for which the density shape is Gaussian.

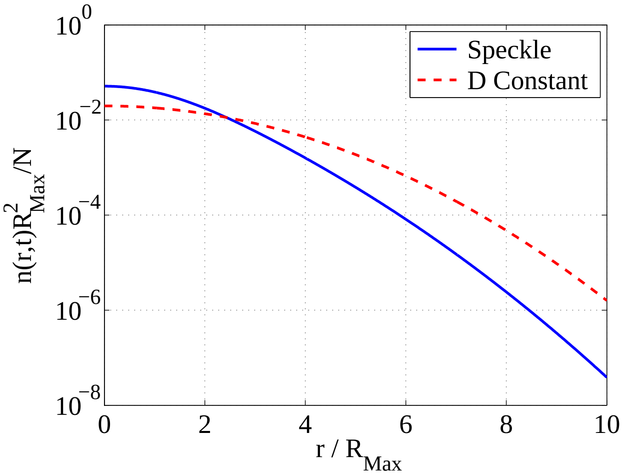

Figure 4: (Color online) Comparison between the Fermi gas density for $2d$ speckle, Eq. (26), and constant diffusion coefficient D, Eq. (29), at $\widetilde{t} = 400$. The parameters are $s = 12$ and $\eta = 0.05$, for which the momentum cutoff $p_c \ll p_F$.

For larger time, such that $r \ll \sqrt{4D_<(k_F)t}$ (i.e. $\widetilde{r} \ll \sqrt{\frac{\widetilde{t}}{\pi s}}$), and for $r > R_{Max}$, Eq.(26), with the help of (27), reduces to

$$\widetilde{n}(\widetilde{r},\widetilde{t}) \approx \frac{2Ns}{\widetilde{t}} \ln \left[\min \left[\frac{\widetilde{t}}{\pi s \widetilde{r}^2}, \frac{1}{2\pi s \eta^2} \right] \right] , \tag{30}$$

which differs from the "usual" large time $1/t$ behavior by the logarithmic factor. The later originates from the diffusion constant dispersion. Finally, for $r > \sqrt{4D_<(k_F)t}$ (and for $r < \frac{4D_<(k_F)t}{R_{max}}$, where (26) is still valid), one can use the large x asymptotic expansion [16]

$$E_1(x) = x^{-1} e^{-x} [1 + O(\frac{1}{x})] \tag{31}$$

to obtain

$$\widetilde{n}(\widetilde{r},\widetilde{t}) \approx \frac{2N\widetilde{t}}{\widetilde{r}^4 s \pi^2} \exp\left(-\frac{\pi s \widetilde{r}^2}{\widetilde{t}} \right) , \tag{32}$$

which differs from the Gaussian decay by the algebraic factor $\frac{1}{\widetilde{r}^4}$. Let us note that this asymptotics is for zero temperature, i.e. when there is a sharp cutoff of the atomic momentum distribution at E_F.

In order for the condition $k_F \ll k_0$ to be fulfilled, the number of atoms N should be fairly small. When N increases, for a fixed frequency trap ω, one arrives to the opposite regime

$k_F \gg k_0$. The integral (23) is then split into two parts (using (20)):

$$n(r,t) = \frac{R_{Max}^2}{8\pi t}\left[\int_{k_c}^{\lambda k_0} \frac{kdk}{D_<(k)} \exp\left(-\frac{r^2}{4D_<(k)t}\right)\left(1-\frac{k^2}{k_F^2}\right) + \right.$$

$$\left. + \int_{\lambda k_0}^{k_F} \frac{kdk}{D_>(k)} \exp\left(-\frac{r^2}{4D_>(k)t}\right)\left(1-\frac{k^2}{k_F^2}\right)\right] \equiv n_<(r,t) + n_>(r,t)\ . \tag{33}$$

The first part, $n_<(r,t)$, describes contribution of "slow" particles which diffuse with the coefficient $D_<(k) \sim k^2$, as in a white noise potential. The second part, $n_>(r,t)$, corresponds to "fast" particles for which correlations in the random potential lead to a sharp increase in the diffusion coefficient, $D_>(k) \sim k^5$. For an arbitrary r, the solution of (33) is given by :

$$\widetilde{n}(\widetilde{r},\widetilde{t}) = \frac{2Ns}{\widetilde{t}}\left(F_1\left(\frac{2\pi\widetilde{r}^2}{\widetilde{t}}\right) + F_2\left(\frac{64}{45\pi}\frac{\widetilde{r}^2}{\widetilde{t}}\right)\right), \tag{34}$$

where

$$F_1(x) = 2\pi s\eta^2 e^{-\frac{x}{4\pi\eta^2}} - \frac{\lambda^2 s}{2}e^{-\frac{x}{\lambda^2}} + \left(1+\frac{sx}{2}\right)\left(E_1\left[\frac{x}{\lambda^2}\right] - E_1\left[\frac{x}{4\pi\eta^2}\right]\right),$$

$$F_2(x) = \frac{64}{225\pi^2}\left[\frac{s}{2}x^{-\frac{1}{5}}\left(\Gamma\left[\frac{1}{5},\frac{x}{\lambda^5}\right] - \Gamma\left[\frac{1}{5},\left(\frac{s}{2}\right)^{\frac{5}{2}}x\right]\right) + x^{-\frac{3}{5}}\left(\Gamma\left[\frac{3}{5},\left(\frac{s}{2}\right)^{\frac{5}{2}}x\right] - \Gamma\left[\frac{3}{5},\frac{x}{\lambda^5}\right]\right)\right]$$

and $\Gamma(\alpha, z)$ is the incomplete Gamma function. In Fig. 5 the density $\widetilde{n}(\widetilde{r},\widetilde{t})/N$ is plotted for $s = \frac{1}{2}$ and $\eta = 0.01$ as a function of the normalized time and distance. One can observe that for fixed r the time evolution of the density exhibits a slight kink. It is due to the division of particles into two groups - "fast" ($k > \lambda k_0$) and "slow" ($k < \lambda k_0$). It is not clear whether this is a genuine physical effect or an artifact of the approximation (20) for $D(k)$.

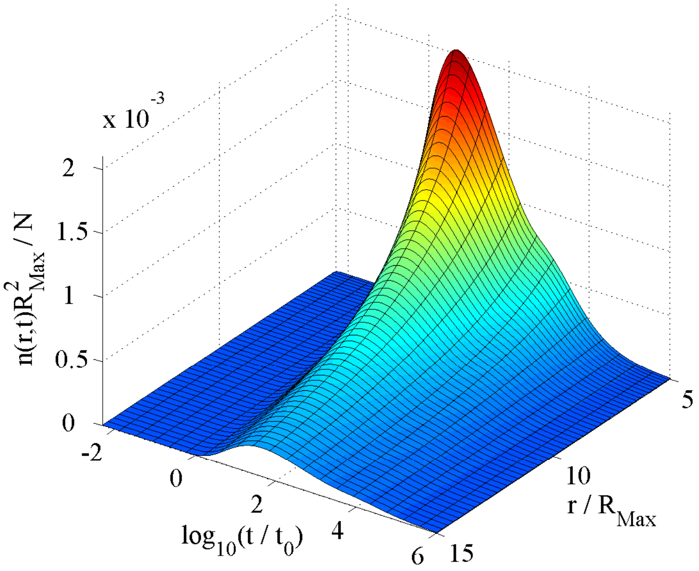

Figure 5: (Color online) Normalized atomic density $\widetilde{n}(\widetilde{r},\widetilde{t})/N$ Eq.(34) as a function of normalized time and distance for $s=\frac{1}{2}$ and $\eta=0.01$.

For $r>\sqrt{4D_>(k_F)t}$, the asymptotic tail of the solution (34) can be written as

$$\widetilde{n}(\widetilde{r},\widetilde{t}) \sim \frac{1}{\widetilde{r}^4}\exp\left(-\beta s^{\frac{5}{2}}\frac{\widetilde{r}^2}{\widetilde{t}}\right), \tag{35}$$

where $\beta=\frac{4}{45\pi\sqrt{2}}$.

The above discussion pertained to the case $\eta \ll 1$. In the opposite case, $\eta \gg 1$, disorder correlations are important for all relevant values of k, so that one should use $D_>(k)$ in the whole region of integration. This is because the weak disorder condition, $kl_B>1$, can now be satisfied only for $k>k_0$, see Eq.(18). The cutoff k_c, below which this condition fails, is now given by $k_c \sim k_0\eta^{\frac{2}{5}}>k_0$. Thus, $n(\vec{r},t)$ is given by the second term in (33), but with the lower limit of integration being equal to k_c.

Let us return to the question of validity of the expression (23). It was argued that the transition from (13) to (26), i.e. the replacement of $P_p(\vec{r},\vec{R},t)$ by $P_p(\vec{r},0,t)$ is justified for sufficiently long time. However, whether a given time t can be considered "sufficiently long" depends on the value of the diffusion coefficient for the relevant particles. It is clear that for "fast" particles, which rapidly diffuse out from the vicinity of the trap, (26) will become accurate at earlier times than for slow particles, which tend to stay in the vicinity of the trap for much longer. Formally, the replacement of $P_p(\vec{r}, \vec{R}, t)$ by $P_p(\vec{r}, 0, t)$ requires

$$\frac{rR_{Max}}{2D(k)t} < 1 \tag{36}$$

and

$$\frac{R_{Max}^2}{4D(k)t} < 1\,. \tag{37}$$

For $r > R_{Max}$ it is sufficient to satisfy only (36), because (37) will be satisfied automatically. Then, for some fixed r one can identify three different time limits. For short times, $t < \frac{rR_{Max}}{2D(k_F)t}$, (36) breaks down. This, however, is of no consequence since at such small times even the fastest particles have not yet arrived to point r (more precisely, particle density there is exponentially small). For intermediate time, $t \sim \frac{r^2}{4D(k_F)}$, the fast particles arrive to point r and the above conditions are satisfied for these particles (these conditions are not satisfied for slow particles but this is irrelevant since, for these r and t, the contribution of slow particles to $n(r,t)$ is small). For longer times, $t > \frac{r^2}{4D(k_F)}$, the fast particles ($k \sim k_F$) have already diffused away and slower particles start to arrive at point r. The arrival time for particles with a given value of k (smaller than k_F) is of order $\frac{r^2}{D(k)}$ so that the condition (36) is satisfied for these particles. It follows, thus, that for $r \gg R_{Max}$ the above conditions are satisfied for the "relevant" particles, i.e. the ones which dominate the concentration at a given r and t.

For $r < R_{Max}$ the more stringent condition is (37) and in order for it to be satisfied for the smallest wave number $k = k_c$, one needs $t > \frac{R_{max}^2}{4D(k_c)}$, i.e. $\widetilde{t} > \frac{1}{\eta^2}$ (we assume here $\eta \ll 1$). In order to obtain more accurate results for $r < R_{Max}$ and for not too long times, one has to return to Eq. (13) and use the kernel $P_p(\vec{r}, \vec{R}, t)$, rather than the long time approximation $P_p(\vec{r}, 0, t)$. It turns out that for $r = 0$ and for the case $k_F \ll k_0$ Eq.(13) can be evaluated exactly for an arbitrary time t:

$$\widetilde{n}(0,\widetilde{t}) = 4Ns\left[\eta^2\left(e^{\frac{\pi s}{\widetilde{t}}-\frac{1}{2\widetilde{t}\eta^2}} - 1\right) + \frac{1}{2\widetilde{t}}e^{\frac{\pi s}{\widetilde{t}}}\left(E_1\left[\frac{\pi s}{\widetilde{t}}\right] - E_1\left[\frac{1}{2\widetilde{t}\eta^2}\right]\right)\right]. \tag{38}$$

For $\widetilde{t} > \pi s$, (38) can be cast in the following form:

$$\widetilde{n}(0,\widetilde{t}) \approx \frac{2Ns}{\widetilde{t}}\left(\ln\left[\min\left[\frac{\widetilde{t}}{\pi s}, \frac{1}{2\pi s\eta^2}\right]\right] + O\left(1\right)\right). \tag{39}$$

It is instructive to compare the above results for $\widetilde{n}(0,\widetilde{t})$ with the solution for the constant diffusion coefficient $D = D_<(k_F)$, which, for $\widetilde{t} > \pi s$, is approximately

$$\widetilde{n}(0,\widetilde{t}) \approx \frac{Ns}{\widetilde{t}}(1 - 2\pi s\eta^2)^2. \tag{40}$$

In the case of the speckle disorder, the decay is slowed down by the factor $2\ln\left[\min\left[\frac{\widetilde{t}}{\pi s},\frac{1}{2\pi s\eta^2}\right]\right]$, reflecting slower diffusion of less energetic particles. As an illustration, in Fig. 6 we compare these two cases for $s = 12$ and $\eta = 0.05$. Note that for $\widetilde{t} > \frac{1}{\eta^2}$, (38) reduces to Eq. (28).

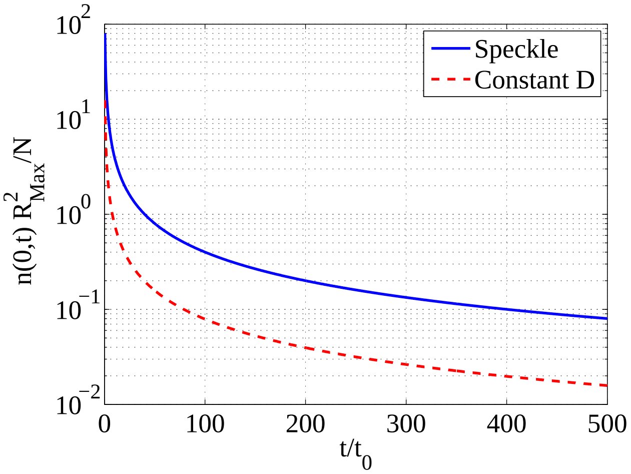

Figure 6: (Color online) Comparison between the Eq.(39) and the corresponding expression for a constant diffusion coefficient Eq.(40), for $s = 12$ and $\eta = 0.05$.

For the case $k_F \gg k_0$ the expression for $\tilde{n}(0,\tilde{t})$ is more cumbersome and involves incomplete Gamma functions. The main differences from the case $k_F \ll k_0$ occurs for times $s^{\frac{5}{2}} \ll \tilde{t} \ll 1$. For such times, the density decays as

$$\tilde{n}(0,\tilde{t}) \sim \tilde{t}^{-\frac{2}{5}}. \tag{41}$$

For larger times, $\tilde{t} \gg 1$, the behavior of the density $\tilde{n}(0,\tilde{t})$ will be generally similar to the case $k_F \ll k_0$, as discussed above.

Finally, let us calculate the variance $\Delta r^2(t) = \int n(\vec{r},t) r^2 d\vec{r}$ of the expanding density profile. Substituting $n(\vec{r},t)$ from (13), we obtain

$$\Delta r^2(t) = \frac{d}{2+2d} R^2_{max} + 2d\bar{D}t\,, \tag{42}$$

where $\bar{D}$ denotes average of $D(p)$ over the momentum distribution:

$$\bar{D} = \frac{2\Gamma(d)}{\pi^{\frac{d}{2}}\Gamma(\frac{d}{2})} \int\limits_{|p|<p_F} \frac{d\vec{p}}{p_F^{2d}} \left(p_F^2 - p^2\right)^{\frac{d}{2}} D(p)\ . \tag{43}$$

Similar result was obtained in Ref.[5] for the variance of the BEC cloud expanding from the harmonic trap. In that case, however, the momentum distribution is given by the inverted parabola in both $d = 2$ and $d = 3$.

V. DIFFUSION OF A BEC

Previous sections were devoted to a cold Fermi gas. In this section we briefly discuss diffusion of a BEC expanding through an optical speckle. This problem has been addressed in a rather detailed and experimentally relevant paper of Miniatura *et al* [5], with an emphasis on the limiting stationary density distribution. Here we concentrate on the earlier stages of the time evolution of the expanding BEC cloud. Our treatment will be within the mean field (Gross-Pitaevskii) approximation, when the BEC can be described by a single macroscopic wave function $\Psi(\vec{r}, t)$. The expansion occurs in two stages, when the first stage is dominated by the nonlinearity whereas the second stage describes a linear evolution in the presence of disorder [4–6, 17]. Initially the condensate is prepared in a harmonic trap (frequency ω) and its energy is dominated by interactions, i.e. by the nonlinear term in the Gross-Pitaevskii equation. At time $t = 0$ the trap is switched off and the BEC undergoes a free (ballistic) expansion for a time t_0 equal to few $(\frac{1}{\omega})$. By that time the interaction energy, stored in the initial wave packet, is converted into the kinetic energy of the condensate flow so that the interaction can be neglected. At $t = t_0$ the random speckle potential is switched on and the BEC evolves according to the linear Schrödinger equation, with the static potential $V(\vec{r})$. It has to be solved with the initial condition $\Psi(\vec{r}, t_0) = \Phi(\vec{r})$, where $\Phi(\vec{r})$ is the condensate wave function at time t_0. Its shape is given by an inverted parabola, with superimposed rapid phase oscillations indicating large kinetic energy (see Eq.(23) of Ref. [5]). Measuring the time from the instant t_0, the standard treatment leads to the following expression for the condensate density, averaged over various realizations of $V(\vec{r})$ (compare to (10)):

$$n_B(\vec{r}, t) = \int d\vec{R} \int d\vec{p} P_p(\vec{r}, \vec{R}, t) W_B(\vec{p}, \vec{R}) \, , \tag{44}$$

where $W_B(\vec{p}, \vec{R})$ is the Wigner function corresponding to the wave function $\Phi(\vec{r})$. Let's compare (44) with the corresponding expression (13) for fermions. Defining the "effective Wigner function" of the Fermi gas as

$$W_F(\vec{p}, \vec{R}) = \frac{1}{(2\pi\hbar)^d} \Theta(E_F - \frac{p^2}{2m} - \frac{1}{2} m\omega^2 R^2) \tag{45}$$

we can write (13) exactly in the form as (44), with W_B replaced by W_F. The two functions have much in common. Integration over $\vec{p}$ and over $\vec{R}$, respectively, shows that the spatial distribution and the momentum distribution for $W_F(\vec{p}, \vec{R})$ are inverted parabolas (in $2d$), with characteristic length $R_{Max} = \frac{\hbar p_F}{m\omega}$ and characteristic momentum p_F. But such inverted parabolas (with k_F replaced by the inverse healing length $1/\xi$ of the BEC prior to the release from the trap) are well known to correspond to the condensate wave function $\Phi(\vec{r})$ and, thus, to the Wigner function $W_B(\vec{p}, \vec{R})$. It is therefore clear that the dynamics of a BEC and of a Fermi cloud must be quite similar. (This similarity has been used in [4] to propose a single parameter scaling for BEC dynamics). For instance, in the long time limit discussed in Sec. IV, when $\vec{R}$ in the diffusion kernel $P_p(\vec{r}, \vec{R}, t)$ can be set to zero, (44) will involve only the momentum distribution $\int d\vec{R} W_B(\vec{p}, \vec{R})$ and, thus, the functional form of $n_B(\vec{r}, t)$ will be identical to that of the Fermi gas. Therefore all the results based on Eq.(23) - such as those given in (25) or (33) - hold also for a BEC (with the replacement $k_F \to 1/\xi$).

One should keep in mind that, in spite of having much in common, the functions $W_B(\vec{p}, \vec{R})$ and $W_F(\vec{p}, \vec{R})$ are not identical (indeed, two Wigner functions with the same spatial and momentum distributions do not necessarily coincide!). Therefore, for $r \lesssim R_{Max}$ (and for not too long times) the shape of a BEC cloud is expected to differ significantly from that of a Fermi gas. Eq.(25) is not applicable in this regime and one should use the more elaborate Eq.(44) which is the bosonic counterpart of Eq.(13) for fermions.

VI. CONCLUSIONS

We have considered diffusion of a Fermi gas in the presence of a random optical speckle potential. The problem, although straightforward in principle, is quite involved technically and it differs in several respects from the standard diffusion problem encountered in condensed matter physics [14]. One difference is that a broad range of particle momenta has to be considered, rather than a narrow interval near the Fermi momentum (as is usually the case for the electronic systems). Another difference is that the speckle potential has long range correlations.

We have emphasized the importance of the parameter $\eta = \frac{V_0}{E_0}$, where V_0 and E_0 are, respectively, the typical amplitude and the "correlation energy" of the potential [18]. For $\eta \ll 1$, particles with wave number $k < k_0$ do not feel correlations in the potential and diffuse as in a white noise potential. For $\eta \gg 1$, on the other hand, correlations are important for all particles, regardless of their momenta. In that case an accurate estimate of the lower cutoff, k_c, below which classical Boltzmann transport is impossible, becomes somewhat ambiguous. Our estimate was based on the Ioffe-Regel criterion, $k_c l_B = 1$, and it leads to $k_c \sim k_0 \eta^{\frac{2}{5}} > k_0$. This corresponds to a critical energy $E_c \sim E_0 \eta^{\frac{4}{5}}$ which is slightly smaller than V_0. Since, however, E_c is much above the percolation threshold E_p (in two dimensions $E_p = 0$), there exists a broad range of energies in which particles can propagate by classical percolation (of course, in $2d$, and at sufficiently large distance, quantum interference will eventually take over and lead to localization). Such "percolating particles" were not accounted for in our treatment. This omission can be partially rectified by treating k_c as a phenomenological fitting parameter whose value is determined from experiment.

Although the paper is devoted primarily to fermions, we have discussed in the last section diffusion of a BEC. It turns out that, within the Gross-Pitaevskii approximation, the shape of a diffusing BEC cloud is remarkably similar to that of a Fermi gas.

All kinds of localization effects have been neglected in the present paper, so that the weak disorder requirement, $k_F l_B \gg 1$, is a necessary condition for the results to be valid. Finally, we have focused on the $2d$ case. Similar calculations can be performed also in $3d$, starting from Eq.(13). Of course, one has to use the $3d$ diffusion kernel and the appropriate expression for the diffusion coefficient $D(k)$ in a $3d$ speckle potential.

---

[1] For a recent reviews see L. Fallani, C. Fort and M. Inguscio, Advances in Atomic, *Molecular and Optical Physics* **56**, 119 (2008); A. Lagendijk, A. van Tiggelen and D.S. Wiersma, "Fifty years of Anderson localization", Phys. Today **62**, 24 (2009); A. Aspect and M. Inguscio, "Anderson localization of ultracold atoms", Phys. Today **62**, 30 (2009); L. Sanchez-Palencia and M. Lewenstein, "Disordered quantum gases under control", arXiv: 0911.0629.

[2] J. Billy, V. Josse, Z. Zuo, A. Bernard, B. Hambrecht, P. Lugan, D. Clément, L. Sanchez-Palencia, P. Bouyer and A. Aspect, *Nature* **453**, 891 (2008).

[3] G. Roati, C. D'Errico, L. Fallani, M. Fattori, C. Fort, M. Zaccanti, G. Modugno, M. Modugno and M. Inguscio, *Nature* **453**, 895 (2008). In this work a quasi-periodic (rather than random) potential was used.

[4] B. Shapiro, *Phys. Rev. Lett.* **99**, 060602 (2007).

[5] C. Miniatura, R.C. Kuhn, D. Delande and C.A. Müller, *Eur. Phys. J. B* **68**, 353 (2009).

[6] S.E. Skipetrov, A. Minguzzi, B.A. van Tiggelen and B. Shapiro, *Phys. Rev. Lett.* **100**, 165301 (2008).

[7] N. Cherroret and S.E. Skipetrov, *Phys. Rev. A* **79**, 063604 (2009).

[8] G. Schwiete and A.M. Finkel'stein, *arxiv:* 0905.4722.

[9] N. Cherroret and S.E. Skipetrov, *Phys. Rev. Lett.* **101**, 190406 (2008).

[10] S. Giorgini, L.P. Pitaevskii and S. Stringari, *Rev. Mod. Phys.* **80**, 1215 (2008).

[11] Y. Castin, in "Ultra-cold Fermi gases", Proc. Inter. School of Physics "Enrico Fermi", Varenna, Eds. M. Inguscio, W. Ketterle and C. Salomon, p.289 (2007).

[12] P. Henseler and B. Shapiro, *Phys.Rev. A* **77**, 033624 (2008).

[13] R.C. Kuhn, O. Sigwarth, C. Miniatura, D. Delande and C.A. Müller, *New Jour. Phys.* **9**, 161 (2007).

[14] E. Akkermans and G. Montambaux, "Mesoscopic Physics of Electrons and Photons", Cambridge University Press (2006).

[15] W. P. Schleich, "Quantum Optics in Phase Space", Wiley (2001).

[16] M. Abramowitz, I. Stegun, "Handbook of mathematical functions with formulas, graphs, and mathematical table", Dover Publications, New York (1972).

[17] L. Sanchez-Palencia, D. Clement, P. Lugan, P. Bouyer, G.V. Shlyapnikov and A. Aspect, *Phys. Rev. Lett.* **98**, 210401 (2007).

[18] This parameter is important also in the opposite regime of strong localization, when the atoms are confined to deep wells of the random potential (see B. I. Shklovskii, Semiconductors (St. Petersburg) **42**, 927 (2008)).